JBM
J Bone Metab 2023;30(1):93-101
https://doi.org/10.11005/jbm.2023.30.1.93
pISSN 2287-6375 eISSN 2287-7029

Original Article

Sphenoid Bone Determines the Curvature of the Cranial Vault in Postnatal Skull Development in C57BL/6 Mice

Dinuka Adasooriya, Minjae Kyeong, Sung-Won Cho

Division of Anatomy and Developmental Biology, Department of Oral Biology, BK21 FOUR Project, Yonsei University College of Dentistry, Seoul, Korea

Corresponding author

Sung-Won Cho
Division of Anatomy and Developmental Biology, Department of Oral Biology, BK21 FOUR Project, Yonsei University College of Dentistry, 50-1 Yonsei-ro, Seodaemun-gu, Seoul 03722, Korea
Tel: +82-2-2228-3065
E-mail: chosome1@yuhs.ac

Received: January 11, 2023
Revised: January 27, 2023
Accepted: February 15, 2023

Background: The skull is a complex structure formed by the craniofacial bones' elaborate organization. The growth pattern in each craniofacial bone of the postnatal skull has been presented in wild-type mice. However, the skull's growth pattern, determined by the craniofacial bones' coordinated growth, is unfamiliar. This study aimed to examine the overall morphological change in the mid-sagittal plane of the postnatal mice's skulls and interaction between the craniofacial bones. **Methods:** Geometric morphometric principal component analysis was performed in the mid-sagittal plane of 31 wild-type mice's skulls from postnatal days 28 to 98. The relationship between the cranial base and cranial vault was investigated by comparing skulls with early fusion and non-fusion of intersphenoid synchondrosis (ISS). **Results:** The cranial vault flattening and sphenoid bone length increased with age. The cranial vault curvature and sphenoid base length showed a positive correlation that was confirmed by comparing the skulls with early fusion and non-fusion of ISS. The sphenoid bone length and cranial vault angle significantly decreased in the skulls with early fusion of ISS compared to non-fusion skulls. **Conclusions:** It is suggested that the cranial vault flattening is sphenoid bone length-induced but cranial vault length-independent during postnatal mice skull development.

Key Words: Mice, inbred C57BL · Skull · Sphenoid bone

INTRODUCTION

The craniofacial skeleton is formed by 2 mechanisms of bone formation; intramembranous bone formation and endochondral bone formation.[1] The cranial base is formed via endochondral bone formation in a manner similar to long bones in the body, while facial bones and cranial vault bones are formed by intramembranous bone formation.

The cranial base contains multiple growth centers called synchondroses, which are made up of mirror-image growth plates.[2,3] Two synchondroses in the anteroposterior mid-sagittal plane of the cranial base; the pre-sphenoid and basisphenoid bones are joined by intersphenoid synchondrosis (ISS), and the sphenooccipital synchondrosis (SOS) joins the basisphenoid and occipital bones. ISS and SOS contribute significantly to the growth of the cranial vault and upper face as

Copyright © 2023 The Korean Society for Bone and Mineral Research

This is an Open Access article distributed under the terms of the Creative Commons Attribution Non-Commercial License (https://creativecommons.org/licenses/by-nc/4.0/) which permits unrestricted non-commercial use, distribution, and reproduction in any medium, provided the original work is properly cited.

Graphical Abstract

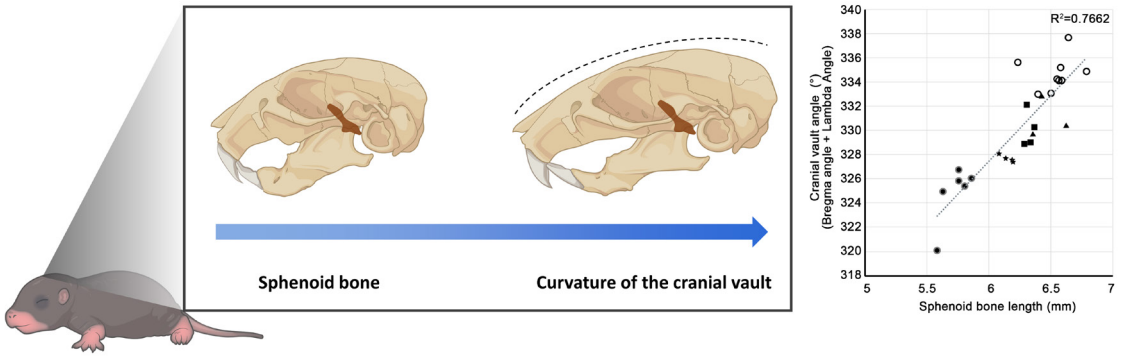

Conclusion It is suggested that the cranial vault flattening is sphenoid bone length-induced but cranial vault length-independent during postnatal mice skull development.

well as the skull base.[2,4] The cranial vault consists of frontal bones, parietal bones, the squamous parts of the temporal bone, and the interparietal part of occipital bone.

The skull is a complex structure formed by the elaborate organization of many bones. Therefore, it was not easy to fully understand the growth of the craniofacial bone. Accurate analysis of craniofacial structures in various mouse models largely depends on an in-depth understanding of the normal craniofacial development of mice. Two recent studies have well-documented the 3-dimensional (3D) metrics of the normal craniofacial development in postnatal skulls in male and female C57BL/6 mice which is one of the most commonly used inbred mouse strains.[2,5,6] It has been suggested that female C57BL/6N mice have generally a very similar craniofacial growth pattern to male C57BL/6J mice.[3] These 2 previous studies presented a reference standard for craniofacial growth of mice up to nearly 4 months of age through a new attempt to place landmarks on the 3D reconstructed skulls using micro-computed tomography (CT) and measure the distance and angle between these landmarks. However, changes in the overall profile of the skull, which are harmoniously created by changes in length and angle, were not presented.

In this study, we performed geometric morphometric analysis of postnatal growth pattern in the mid-sagittal skulls of C57BL/6N mice from postnatal day (P) 28 to P98, and found 2 distinct geometric morphometric changes in the angle of the cranial vault and the length of sphenoid bone. We also found a close relationship between the cranial vault and the sphenoid bone, and tried to verify the relationship.

METHODS

1. Animals

All animal experiments were performed under approved protocols of the Intramural Animal Use and Care Committee of the College of Dentistry, Yonsei University. C57BL/6N mice were euthanized utilizing CO_2 exposure at selected postnatal ages (P28 mice N=6, P42 mice N=4, P63 mice N=4, P70 mice N=4, P98 non-fusion mice N=8, P98 early fusion mice N=5). The number of mice per stage was determined based on previous C57BL/6 mouse studies, all of which used 4 mice per stage.[3,5] We used a minimum of 4 mice per stage in the present study.

2. Micro-CT and reconstruction

Micro-CT images of the fixed mouse skulls were obtained using a micro-CT scanner (Skyscan1173; Bruker-CT, Kontich, Belgium) at 130 kV and 60 μA and were reconstructed using NRecon (Version 1.6; Bruker-CT) with consistent parameters (Fig. 1A).

https://doi.org/10.11005/jbm.2023.30.1.93

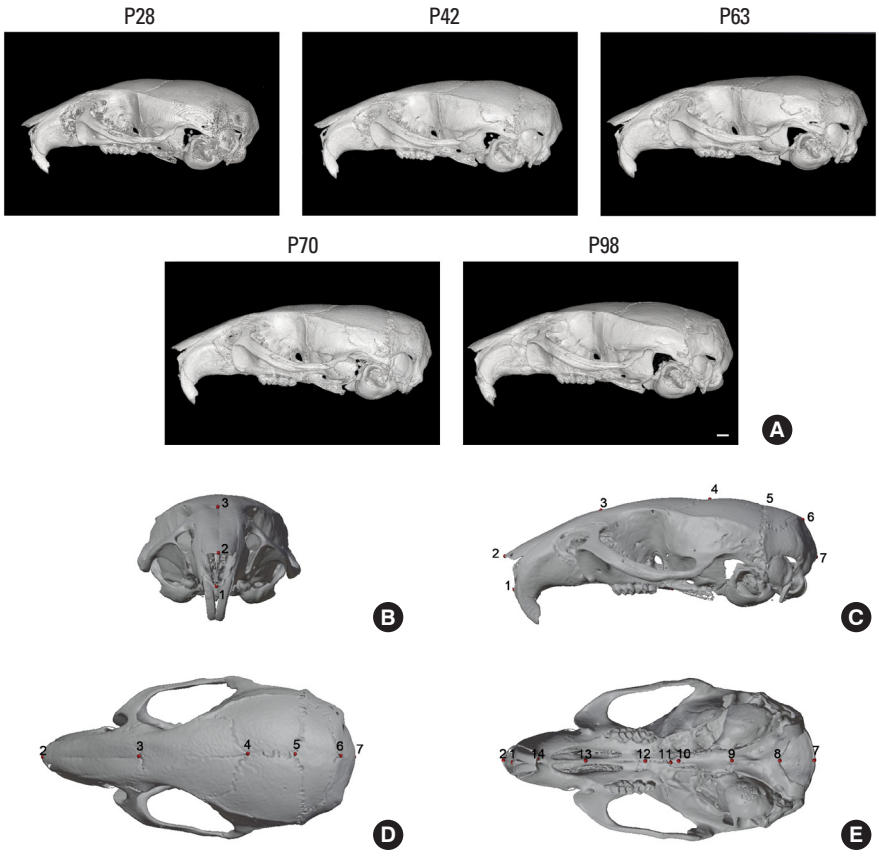

Fig. 1. Lateral view of C57BL/6 mouse skulls and landmarks in the mid-sagittal plane of the skull. (A) Three-dimensional reconstructed skulls at postnatal day (P) 28, P42, P63, P70, and P98. (B-E) The skull with landmarks is viewed from various directions; frontal (B), lateral (C), dorsal (D), and ventral view (E). The 14 landmarks, which are placed in the mid-sagittal plane of the skull, corresponding to landmarks in Table 1. Scale bar =1 mm.

The reconstructions were converted to 3D volumes using the software 3D Slicer (Version 4.1; http://www.slicer.org; Harvard Medical School, Boston, MA, USA). Linear measurements and angular measurements were measured using the micro-CT files by using Blender and OnDemand-3D™ (Version 1.0; CyberMed Inc., Daejeon, Korea).

3. Landmark-based geometric morphometric analysis

The 14 landmarks (Fig. 1B and Table 1) were positioned in the mid-sagittal plane of the 3D skulls using the software Blender (Version 3.2.1; Blender Foundation, Amsterdam, the Netherlands), and the values of the 3D coordinates were exported. All of these landmarks were described previously.[5-8] Principal component (PC) analysis is a widely used multivariate analysis method based on geometric morphometric data to reveal systematic covariations among a group of variables after removing size factor be-

Table 1. Landmark placed in the mid-sagittal plane of mouse skull

No. of landmark	Landmark definition
1	Anterior nasal spine
2	Rhinion
3	Nasion
4	Bregma
5	The intersection of parietal bones with anterior aspect of interparietal bone, midline
6	The intersection of interparietal bone with squamous portion of occipital bone, midline
7	Opisthion
8	Basion
9	The central point of spheno-occipital synchondrosis
10	The central point of intersphenoidal synchondrosis
11	Rostral end of the curvature of the palatine bone (lamina horizontalis ossis palatine)
12	The intersection of the maxillo-palatine suture in the midline
13	Posterior end of the wing of vomer
14	The central point on the premaxilla between the incisors

tween samples. We conducted PC analysis on procrustes shape coordinates for mid-sagittal skulls using the software MorphoJ (Klingenberg Lab, Manchester, UK).

2. Statistics

The correlations were calculated as the coefficient of determination (R2) value by Excel (Microsoft Corp., Redmond, WA, USA). The difference in bone length between groups in each parameter was tested statistically with Mann–Whitney U test using SPSS (version 26.0; IBM Corp., Armonk, NY, USA). All *P*-values of less than 0.05 were considered significant.

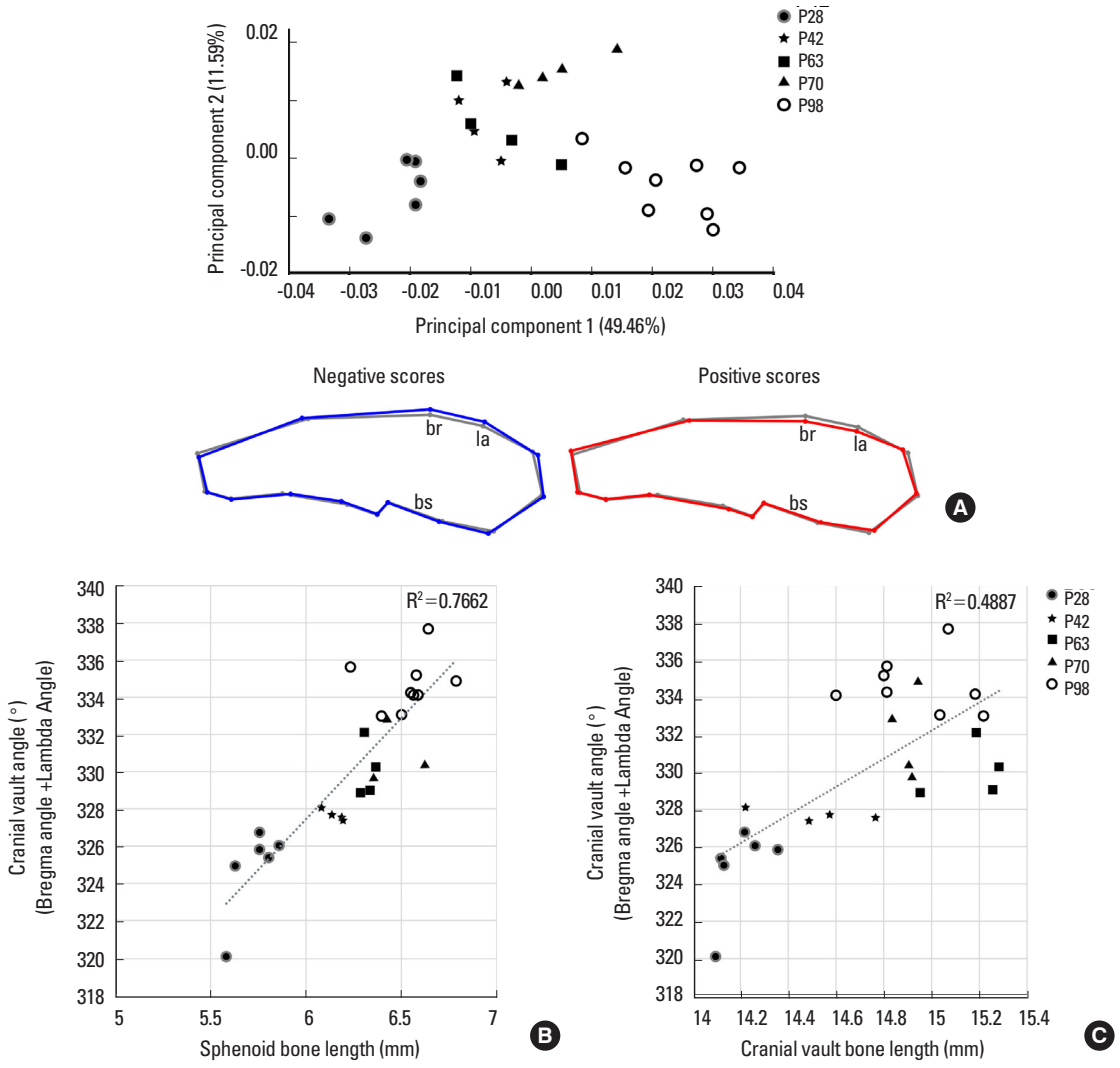

Fig. 2. Geometric morphometric changes in the mid-sagittal skull of the postnatal mice. (A) Principal component (PC) analysis based on procrustes coordinates of 14 cranial mid-sagittal landmarks is presented as scatter plots of individual scores along the PC1 and PC2. The PC 1 explains 49.46% of total shape variance. Skulls from the same age group are well clustered. The postnatal day 28 skulls are located on the left, and the skulls with age gradually moved further to the right along the PC1 axis. The gray wireframe shows the spatial relationships of the landmarks represented at all PC values of 0. Skull with negative PC1 scores (blue wireframe) exhibit a cranial vault that is more curved than average, whereas skulls with positive PC1 scores (red wireframe) exhibit the flatter cranial vault. In addition, the basisphenoid bone of the skull gradually becomes longer as the PC1 score increase. Therefore, a positive score for PC1 corresponds to a polygon composed of a flatter cranial vault and a longer sphenoid bone length. (B) The angles at the bregma and lambda landmarks were summed and regarded as the cranial vault angle. The sphenoid bone length shows a positive correlation with the cranial vault angle ($R^2=0.7662$). (C) There is no direct relationship between cranial vault bone length (total of the frontal, parietal, and interparietal bone length) and the cranial vault angle ($R^2=0.4887$).

https://doi.org/10.11005/jbm.2023.30.1.93

RESULTS

1. The cranial vault angle is closely related with the sphenoid bone length

To investigate the postnatal growth pattern in the mid-sagittal skulls of C57BL/6N mice, a 3D geometric morphometric analysis was performed in skulls at P28, P42, P63, P70, and P98 (Fig. 2A). PC analysis shows that skulls from the same group were well clustered. The youngest skulls were located on the left, and the older skulls showed a higher PC1 value on a PC plot. Skulls of older mice scoring a positive value for PC1 exhibited the flatter cranial vault and the longer sphenoid bone length. PC1 was positively correlated with the centroid size of skulls ($R^2=70.68\%$, $P<0.0001$). There were no significant changes in the length of the cranial vault bones and occipital bone in the PC analysis. In the facial region, the position of the nasal bone tip changed, but there was no significant change in the curvature or length of overall facial bones. Based on the finding that the cranial vault flattening and the sphenoid bone length increased with age, we focused on the cranial vault and skull base in this study.

Furthermore, we investigated the correlation between the curvature of the cranial vault and the length of sphenoid bone. To quantify the curvature of the cranial vault, we measured and summed the angles at bregma and lambda, the 2 points with the most prominent positional change in PC analysis. We found that the cranial vault curvature and sphenoid base length had a positive correlation ($R^2=0.7662$) (Fig. 2B). On the other hand, there is no direct relationship between the cranial vault angle and cranial vault bone length ($R^2=0.4887$) (Fig. 2C). These results indicate that the curvature of the cranial vault was positively correlated with the length of the sphenoid bone, but not with the length of the cranial vault.

2. The cranial vault is domed in mouse skulls with early fusion in the ISS

To confirm the positive correlation between cranial vault curvature and sphenoid base length, a 3D geometric morphometric PC analysis was performed in the mid-sagittal skulls showing early fusion of ISS. Five skulls showing early fusion of ISS were obtained at P98 mice, but we could not find skulls with early fusion of SOS at P98 mice. The skulls with the early fusion of ISS show a domed cranial vault compared to non-fusion skulls (Fig. 3A, B), a complete fusion between presphenoid and basisphenoid bone (Fig. 3C, E).

In PC analysis, the early fusion skulls were clustered on the left along the PC1 value on a PC plot, and the non-fusion skulls were clustered on the right (Fig. 4A). The early fusion skulls with negative scores of PC1 showed domed cranial vault and a shorter sphenoid bone length. PC1 is positively correlated with the centroid size for all the skulls ($R^2=92.33\%$, $P<0.0001$). There were no significant changes in the length of the cranial vault bones, occipital bone and facial bones in the PC analysis. This result means that the cranial vault curvature and the sphenoid bone length are closely related and that sphenoid bone length and the cranial vault angle were significantly decreased in the ISS early fusion skulls compared to non-fusion skulls (Fig. 4B, C).

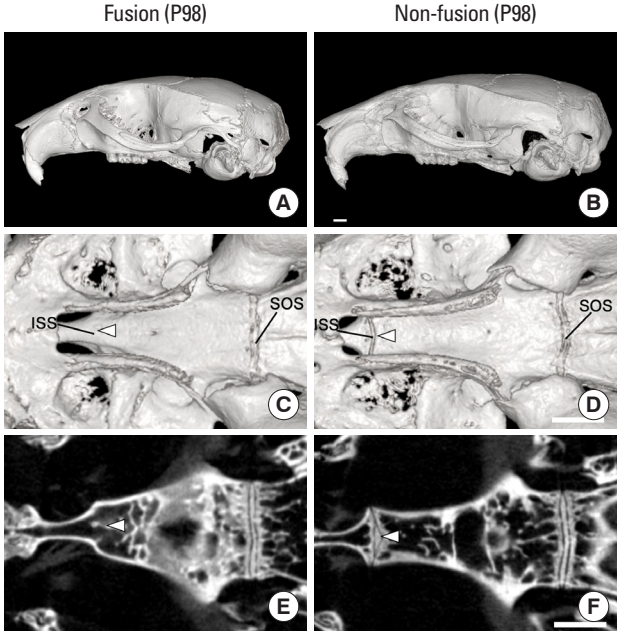

Fig. 3. Mouse skulls with early fusion and non-fusion in intersphenoid synchondrosis (ISS). (A, B) Lateral view of 3-dimensional ISS reconstructed skulls at postnatal day 98. The skull with the early fusion of ISS shows a domed cranial vault compared to the non-fusion skull. (C, D) The dorsal view of early fusion and non-fusion skull. The skull with the early fusion of ISS shows a complete fusion between presphenoid bone and basisphenoid bone. (E, F) In the longitudinal section of the cranial base, early fusion of ISS with poor demarcation in the ISS compared to the non-fusion skull.

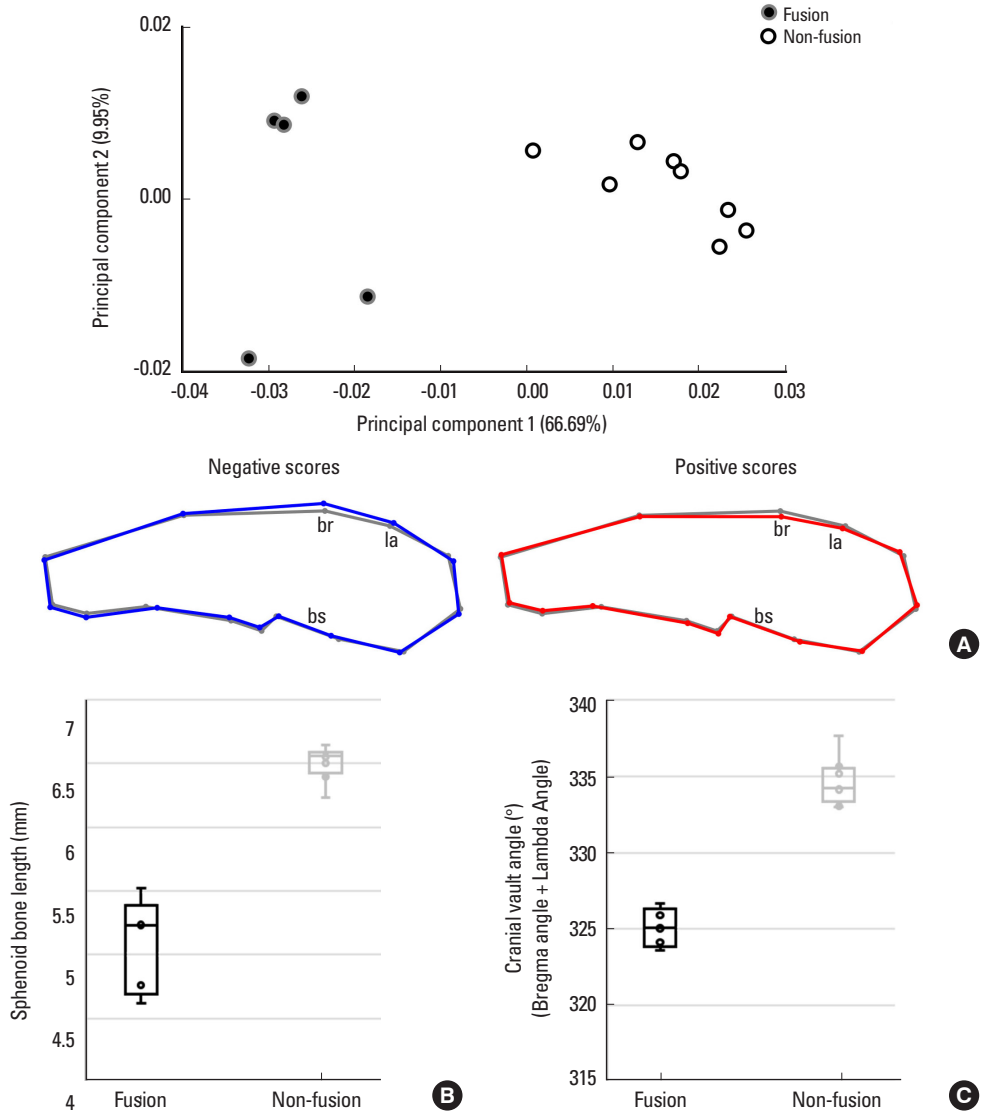

Fig. 4. Geometric morphometric changes in the mid-sagittal skulls with an early fusion of intersphenoid synchondrosis (ISS) and non-fusion skulls. (A) Skulls from the same age group are well clustered. The principal component (PC) 1 explains 66.98% of total shape variance. The early fusion skulls with negative scores of PC1 (blue wireframe), which corresponds to a polygon composed of a domed cranial vault and a shorter sphenoid bone length. The gray wireframe shows the spatial relationships of the landmarks represented at all PC values of 0. (B, C) The ISS early fusion skulls show a significant decrease in the sphenoid bone length and the cranial vault angle summed with the angles at bregma and lambda compared to those of non-fusion skulls in the box plots ($P < 0.005$).

DISCUSSION

To investigate the postnatal growth pattern in the midline of C57BL/6 mouse skulls, the geometric morphometric analysis was performed in the mid-sagittal skulls at P28, P42, P63, P70, and P98. We excluded skulls between p7 and P21, which have been reported to show a rapid change in all dimensions of the skull.[3,5]

1. Relationship between cranial vault angle and sphenoid bone length

We found that the cranial vault flatness and the sphenoid bone length in the mid-sagittal skulls increased with age and that the cranial vault curvature was positively correlated with the sphenoid bone length but not with the cranial vault length. These results are consistent with the result of previous reports.[2,3,5,6] The mid-sagittal angles

https://doi.org/10.11005/jbm.2023.30.1.93

in cranial vault continuously increase until P90 [2] and the cranial base growth in the anteroposterior dimension completely stops after P120.[3,5,6] There is no significant length change in the bones of the cranial vault between P60 and P120.[3] Furthermore, it has been suggested in previous studies that the ISS and SOS in the cranial base contribute significantly to the growth of the cranial vault.[2,4] Similar to this, in the present study, it is suggested that the sphenoid bone contributes to the cranial vault curvature.

2. Contribution of the ISS in cranial vault curvature

To confirm the correlation between cranial vault curvature and sphenoid base length, we compared skulls with early fusion and non-fusion of ISS. The fusion time of ISS and SOS was reported in previous studies. The ISS completely fused sometime after P120 [5] or after P180,[3] and the SOS completely disappeared at P390.[3] In this study, we could obtain 5 wild-type skulls with early fusion of the ISS at P98. A geometric morphometric PC analysis in the present study showed the shorter sphenoid bone length and the more curved cranial vault in the ISS early fusion skulls compared to non-fusion skulls. In many mouse mutants with premature fusion of ISS or SOS, such as *Col2a1-Cre;Fgfr2IIIc* ^{P253R}, *Fgfr2IIIc* $^{-/-}$, *Fgfr2c* $^{C342Y/+}$, *Fgfr3* $^{P244R+/-}$, *Fgfr* $^{3G369C/G369C}$, *Dermo1-Cre;Pkd* $^{-/-}$, *Wnt1-Cre;Pkd2* $^{-/-}$, *Col2a1-Cre;IFT8* $^{-/-}$, *Dermo-Cre;POR* $^{-/-}$, *Alpl* $^{-/-}$, and *BALB/c-* $^{bm/bm}$ mice, domed cranial vaults were accompanied.[9-20] Especially, *Col2a1-Cre; Fgfr2IIIc* ^{P253R} and *Col2a1-Cre;IFT8* $^{-/-}$ mice, whose mutations are controlled by a cartilage-specific promoter in the cranial base, exhibited a premature fusion of ISS or SOS and a domed cranial vault together.[9,17] Based on results of wild-type mice in the present study and mutant mice in previous studies, it is suggested that the cranial vault flattening is driven by the sphenoid bone lengthening, but is independent of the cranial vault length during postnatal mouse skull development.

The data from C57BL/6 mice in the present study are unlikely to be directly applicable to humans because there are striking morphological differences between human and mouse skull bases. First, the overall shape of the sphenoid bone is completely different between humans and mice. In the lateral view, the body of the sphenoid bone is curved in humans and the sphenoid bone in mice is flat. Due to these differences, the angle at the base of the skull is highly flexed at an acute angle in humans. On the other hand, the skull base angle is retroflexed (>180° when measured ventrally) in mice, just as it is flat or obtuse in most mammals.[21] Second, the postnatal cranial base angle decreases in mice,[3,5] but increases in humans.[21] It has been suggested that cranial base flexion contributes more than the cranial base length to allow a larger cranial volume in humans.[22] Furthermore, it is very difficult to fully establish the developmental pattern of the human skull due to environmental factors and high genetic heterogeneity.[23] In this respect, skull studies in highly inbred mouse strains are meaningful in that they can provide a clue to understanding mammalian skull development patterns based on genetic diversity and minimization of environmental factors within the strain. Similar to this, further studies are needed to determine whether the data from C57BL/6 mice in the present study apply equally to other mouse strains, since a previous study examining the skull morphology of C57BL/6, BALB/cA, C3H/HeJ, CBA/JNCr, ICR, MSM/Ms, and Mus spretus indicated that the skull morphology was highly variable between mouse strains and clearly geometrically distinguishable.[24]

DECLARATIONS

Funding

This work was supported by the National Research Foundation of Korea (NRF) grant funded by the Korea government (MSIT). (No.2020R1A2C2005790).

Ethics approval and consent to participate

All animals were treated in accordance with the Guide for the Intramural Animal Use and Care Committee of the College of Dentistry, Yonsei University.

Conflict of interest

No potential conflict of interest relevant to this article was reported.

ORCID

Dinuka Adasooriya *https://orcid.org/0000-0002-8413-8247*
Minjae Kyeong *https://orcid.org/0000-0003-0174-0812*
Sung-Won Cho *https://orcid.org/0000-0001-7505-9769*

REFERENCES

1. Kronenberg HM. Developmental regulation of the growth plate. Nature 2003;423:332-6. https://doi.org/10.1038/nature01657.
2. Wei X, Hu M, Mishina Y, et al. Developmental regulation of the growth plate and cranial synchondrosis. J Dent Res 2016;95:1221-9. https://doi.org/10.1177/0022034516651823.
3. Wei X, Thomas N, Hatch NE, et al. Postnatal craniofacial skeletal development of female C57BL/6NCrl mice. Front Physiol 2017;8:697. https://doi.org/10.3389/fphys.2017.00697.
4. Hoshino Y, Takechi M, Moazen M, et al. Synchondrosis fusion contributes to the progression of postnatal craniofacial dysmorphology in syndromic craniosynostosis. J Anat 2023;242:387-401. https://doi.org/10.1111/joa.13790.
5. Vora SR, Camci ED, Cox TC. Postnatal ontogeny of the cranial base and craniofacial skeleton in male C57BL/6J mice: A reference standard for quantitative analysis. Front Physiol 2015;6:417. https://doi.org/10.3389/fphys.2015.00417.
6. Maga AM, Navarro N, Cunningham ML, et al. Quantitative trait loci affecting the 3D skull shape and size in mouse and prioritization of candidate genes in-silico. Front Physiol 2015;6:92. https://doi.org/10.3389/fphys.2015.00092.
7. Macholán M, Mikula O, Vohralík V. Geographic phenetic variation of two eastern-Mediterranean non-commensal mouse species, Mus macedonicus and M. cypriacus (Rodentia: Muridae) based on traditional and geometric approaches to morphometrics. Zool Anz 2008;247:67-80. https://doi.org/10.1016/j.jcz.2007.07.003.
8. Singh N, Dutka T, Devenney BM, et al. Acute upregulation of hedgehog signaling in mice causes differential effects on cranial morphology. Dis Model Mech 2015;8:271-9. https://doi.org/10.1242/dmm.017889.
9. Nagata M, Nuckolls GH, Wang X, et al. The primary site of the acrocephalic feature in Apert Syndrome is a dwarf cranial base with accelerated chondrocytic differentiation due to aberrant activation of the FGFR2 signaling. Bone 2011;48:847-56. https://doi.org/10.1016/j.bone.2010.11.014.
10. Eswarakumar VP, Horowitz MC, Locklin R, et al. A gain-of-function mutation of Fgfr2c demonstrates the roles of this receptor variant in osteogenesis. Proc Natl Acad Sci USA 2004;101:12555-60. https://doi.org/10.1073/pnas.0405031101.
11. Eswarakumar VP, Monsonego-Ornan E, Pines M, et al. The IIIc alternative of Fgfr2 is a positive regulator of bone formation. Development 2002;129:3783-93. https://doi.org/10.1242/dev.129.16.3783.
12. Perlyn CA, DeLeon VB, Babbs C, et al. The craniofacial phenotype of the Crouzon mouse: analysis of a model for syndromic craniosynostosis using three-dimensional MicroCT. Cleft Palate Craniofac J 2006;43:740-8. https://doi.org/10.1597/05-212.
13. Laurita J, Koyama E, Chin B, et al. The Muenke syndrome mutation (FgfR3P244R) causes cranial base shortening associated with growth plate dysfunction and premature perichondrial ossification in murine basicranial synchondroses. Dev Dyn 2011;240:2584-96. https://doi.org/10.1002/dvdy.22752.
14. Chen L, Adar R, Yang X, et al. Gly369Cys mutation in mouse FGFR3 causes achondroplasia by affecting both chondrogenesis and osteogenesis. J Clin Invest 1999;104:1517-25. https://doi.org/10.1172/jci6690.
15. Kolpakova-Hart E, McBratney-Owen B, Hou B, et al. Growth of cranial synchondroses and sutures requires polycystin-1. Dev Biol 2008;321:407-19. https://doi.org/10.1016/j.ydbio.2008.07.005.
16. Khonsari RH, Ohazama A, Raouf R, et al. Multiple postnatal craniofacial anomalies are characterized by conditional loss of polycystic kidney disease 2 (Pkd2). Hum Mol Genet 2013;22:1873-85. https://doi.org/10.1093/hmg/ddt041.
17. Ochiai T, Nagayama M, Nakamura T, et al. Roles of the primary cilium component Polaris in synchondrosis development. J Dent Res 2009;88:545-50. https://doi.org/10.1177/0022034509337775.
18. Panda SP, Guntur AR, Polusani SR, et al. Conditional deletion of cytochrome p450 reductase in osteoprogenitor cells affects long bone and skull development in mice recapitulating antley-bixler syndrome: role of a redox enzyme in development. PLoS One 2013;8:e75638. https://doi.org/10.1371/journal.pone.0075638.
19. Liu J, Nam HK, Campbell C, et al. Tissue-nonspecific alkaline phosphatase deficiency causes abnormal craniofacial bone development in the Alpl(-/-) mouse model of infantile hypophosphatasia. Bone 2014;67:81-94. https://doi.org/10.1016/j.bone.2014.06.040.
20. Tsukamoto Y, Kajii TS, Oonishi Y, et al. Growth and development of the cranial base in mice that spontaneously develop anterior transverse crossbite. Am J Orthod Dentofacial Orthop 2008;134:676-83. https://doi.org/10.1016/

j.ajodo.2006.08.025.
21. Lieberman DE, Hallgrímsson B, Liu W, et al. Spatial packing, cranial base angulation, and craniofacial shape variation in the mammalian skull: testing a new model using mice. J Anat 2008;212:720-35. https://doi.org/10.1111/j.1469-7580.2008.00900.x.
22. Lieberman DE, Ross CF, Ravosa MJ. The primate cranial base: ontogeny, function, and integration. Am J Phys Anthropol 2000;Suppl 31:117-69. https://doi.org/10.1002/1096-8644(2000)43:31+<117::aid-ajpa5>3.3.co;2-9.
23. Vora SR. Mouse models for the study of cranial base growth and anomalies. Orthod Craniofac Res 2017;20 Suppl 1:18-25. https://doi.org/10.1111/ocr.12180.
24. Kawakami M, Yamamura K. Cranial bone morphometric study among mouse strains. BMC Evol Biol 2008;8:73. https://doi.org/10.1186/1471-2148-8-73.